

# Analysis of Displacements of GPA in Normally Consolidated Soft Soil

## L'analyse des déplacements des GPA dans le sol mou Normalement consolidé

Vidyaranya B.

Research Scholar, Osmania University, Hyderabad, India

Madhav M.R.

Professor Emeritus, JNT University, & I.I.T., Hyderabad, India

**ABSTRACT:** Granular piles (GP) offer most effective and economical solution for ground improvement due to their drainage, densification and reinforcement actions, GPs mitigate liquefaction induced damages. An anchor placed at the base of the granular pile and attached to the footing by a cable or rod transfers the applied pullout force to the bottom of the GP termed as Granular Pile Anchor (GPA). The effective stresses in a normally consolidated saturated soil increase linearly with depth. Consequently, the undrained strength and the deformation modulus of the soil increase linearly with depth. Analysis of the displacements of granular pile anchor is presented considering the influence of the linearly increasing undrained modulus of soil and of the GPA with depth on the load – displacement response of the GPA. A parametric study quantifies effects of the length to diameter ratio of GPA, and the relative stiffness of the GP with respect to that of in situ soil at ground level, on the variations of tip and top displacements of GPA with applied load, variation of shear stresses and pullout load with depth, etc.

**RÉSUMÉ :** Pieux granulaires (GP) offrent une solution plus efficace et économique pour amélioration des sols en raison de leur drainage, la densification et des actions de renforcement, les médecins généralistes atténuer les dommages induits par liquéfaction. Un point d'ancrage placé à la base du pieu granulaire et fixée à la semelle par un câble ou une tige transfère la force de traction appliquée sur le fond de la GP qualifiée de mouillage pieu granulaire (GPA). Les contraintes effectives dans un sol normalement consolidé saturé augmente linéairement avec la profondeur. Par conséquent, la résistance non drainée et le module de déformation du sol augmente linéairement avec la profondeur. L'analyse des déplacements de l'ancrage empiement granulaire est présentée compte tenu de l'influence de plus en plus le module linéaire non drainée du sol et de l'GPA avec la profondeur de la réponse force - déplacement du GPA. Une étude paramétrique de quantifier les effets de la longueur par rapport au diamètre de l'GPA, et la rigidité relative du GP par rapport à celle du sol in situ au niveau du sol, sur les variations de pointe et des déplacements supérieurs de GPA avec la charge appliquée, la variation de cisaillement contraintes et la charge de retrait avec la profondeur, etc

**KEYWORDS:** Granular pile anchor, modulus of deformation, homogenous ground, displacements, load transfer.

### 1 INTRODUCTION.

Granular piles (GP) offer most effective and economical solutions in soft marine clays to counter-act low undrained shear strength and stiffness of the deposits. GPs improve the performance of ground by reinforcement, densification, increasing bearing capacity and resistance to liquefaction by increasing strength and stiffness of ground. GPs are ideally suited as they form elements of low compressibility and high shear strength. The effective stresses in a normally consolidated saturated soil increase linearly with depth. As a result the undrained shear strength and deformation modulus of the soil also increase linearly with depth. The increase in modulus of soil and granular material with depth result in reduced load-displacements response and increased confinement pressure.

The functional utility of the GP in compression is extended by placing an anchor at its base to transfer the pullout load or uplift forces to the base and the assembly is termed as Granular Pile Anchor (GPA). Granular pile treated expansive soil adjusts itself to changes in moisture better than an untreated-soil (Phani Kumar *et al.*, 2004). White *et al.* (2001) studied the application of reinforced geopiers for resisting tensile loads and settlement control. Lillis *et al.* (2004) reported results from in situ tests on pullout response of GPA. Kumar *et al.* (2004) present results from laboratory and field tests on pullout response of GPA in cohesive and cohesionless soils. A linear analysis of displacements of GPA is presented by Madhav *et al.* (2008).

### 2 PROBLEM DEFINITION

A granular pile of length,  $L$ , and diameter,  $d$ , with the soil and pile material characterized by moduli of deformation  $E_s$  and  $E_{gp}$ , and unit weights of  $\gamma_s$  and  $\gamma_{gp}$ , respectively is considered (Fig.1). A force,  $P_o$ , applied at the base of GPA is resisted by the shear stress,  $\tau$ , acting along the periphery of the pile. The force and the stresses acting on the GPA are depicted in Figure 2a. The stresses transferred to the in situ soil are shown in Figure. 2b. The non-homogeneities of deformation moduli of soil,  $E_s$  and granular material,  $E_{gp}$  (Fig. 3 & 4) are defined by the parameters,  $\alpha_s$  &  $\alpha_{gp}$ , to quantify the rate of increase of deformation moduli of in-situ soil and granular material with depth. The Poisson's ratio of the soil is  $\nu_s$ . In order to evaluate the upward displacements of the elements of the soil adjacent to the GPA

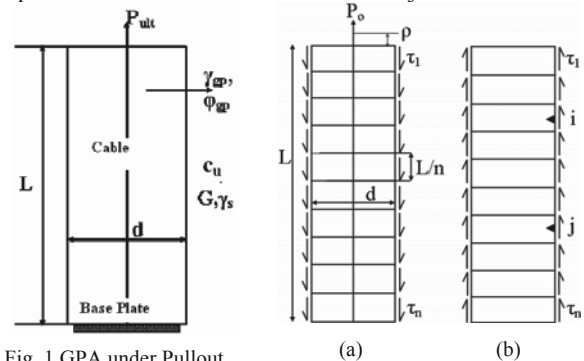


Fig. 1 GPA under Pullout

Fig. 2 Forces and Stresses acting on GPA and Soil.

due to the boundary stresses,  $\tau$ , the GPA surface is divided in to 'n' elements of length,  $\Delta L (=L/n)$ . The stress acting on a typical

element, j, is  $\tau_j$ . The displacement at the centre of an element, i, due to stresses acting on element, j, are obtained by the method described by Poulos and Davis (1980).

Integrating numerically, the Mindlin's equation for a point load in the interior of a semi-infinite elastic continuum over the cylindrical periphery of the element, the displacement,  $\rho_{s,ij}$ , of the soil adjacent to the centre of the i<sup>th</sup> element due to stress,  $\tau_j$ , acting on the element, j, considering deformation modulus,  $E_s$ , of the soil, increases linearly with the depth as

$$E_s(z) = E_{s0} \left( 1 + \alpha_s \frac{z}{L} \right) \text{ is obtained as} \quad (1)$$

$$\rho_{s,ij} = \frac{d}{E_{s0}} \cdot \frac{I_{s,ij}}{\left( 1 + \alpha_s \cdot \left( \frac{z_i}{L} \right) \right)} \cdot \tau_j$$

where  $I_{s,ij}$  – is the soil displacement influence coefficient. The total soil displacement,  $\rho_{s,i}$ , adjacent to node 'i' due to stresses on all the elements of the GPA, is obtained by summing up all the displacements at node 'i', as

$$\rho_{s,i} = \frac{d}{E_{s0}} \sum_{j=1}^n \frac{I_{s,ij}}{\left( 1 + \alpha_s \cdot \left( \frac{z_i}{L} \right) \right)} \tau_j \quad (2)$$

The vertical soil displacements adjacent to all the nodes are collected to arrive at

$$\{\rho_s\} = \frac{d}{E_{s0}} [I_s'] \{\tau\} \quad (3)$$

where  $\{\rho_s\}$  and  $\{\tau\}$  are respectively the soil displacement and stress vectors of size, n, and elements of the matrix  $[I_s']$  are  $I_{s,ij} = \frac{I_{s,ij}}{\left( 1 + \alpha_s \cdot \left( \frac{z_i}{L} \right) \right)}$  - non-dimensional soil displacement influence coefficient of GPA, where  $Z'_i = \frac{z_i}{L}$  - normalized depth at i<sup>th</sup> element.

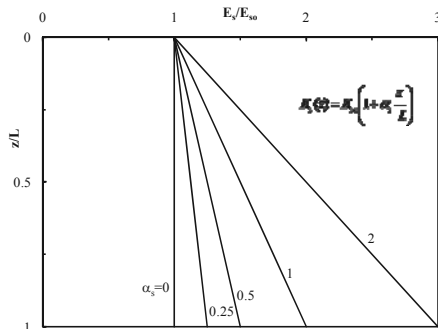


Fig. 3 Variation of  $E_s$  with Depth – Effect of  $\alpha_s$

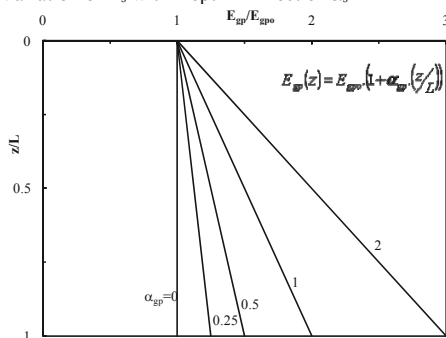


Fig. 4 Variation of  $E_{gp}$  with Depth – Effect of  $\alpha_{gp}$

### 2.1 DISPLACEMENTS OF GPA

The vertical displacements of GPA are obtained considering it to be compressible. Figure 5 depicts the stresses on an infinitesimal element of GPA of thickness,  $\Delta z$ . Poulos and Davis (1980) have established that lateral/radial stresses have negligible effect on the vertical displacements. Considering the deformation modulus of the granular material,  $E_{gp}$ , to increase linearly with depth, z, as

$$E_{gp}(z) = E_{gp0} \left( 1 + \alpha_{gp} \cdot \left( \frac{z}{L} \right) \right) \quad (4)$$

The equilibrium of forces in the vertical direction reduces to

$$\frac{d\sigma_z}{dz} + \frac{4}{d} \tau = 0 \quad (5)$$

where  $\sigma_z$  is the normal stress in to the GPA. The stress-strain relationship for GPA material, is

$$\sigma_z = E_{gp} \cdot \epsilon_z = -E_{gp} \cdot \frac{d\rho_{gp}}{dz} \quad (6)$$

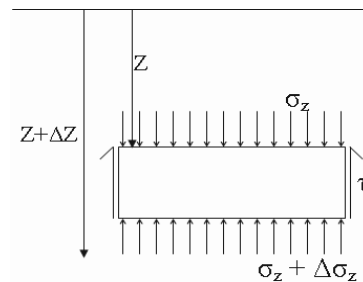


Fig. 5 Stresses acting on an Infinitesimal Element

where  $\epsilon_z$  and  $\rho_{gp}$  are respectively the axial strain and GPA displacement. Substituting for modified  $E_{gp}$  the stress-strain Equation 6 is modified as

$$\sigma_z = E_{gp} \cdot \epsilon_z = -E_{gp0} \left( 1 + \alpha_{gp} \cdot \left( \frac{z}{L} \right) \right) \cdot \frac{d\rho_{gp}}{dz} \quad (7)$$

Differentiating Equation 7 with respect to depth, z,

$$\frac{d\sigma_z}{dz} = -E_{gp0} \left[ \left( \frac{\alpha_{gp}}{L} \right) \frac{d\rho_{gp}}{dz} - E_{gp0} \left( 1 + \alpha_{gp} \cdot \left( \frac{z}{L} \right) \right) \cdot \frac{d^2\rho_{gp}}{dz^2} \right] \quad (8)$$

On simplification the differential Equation 8 becomes

$$\frac{d\sigma_z}{dz} = -E_{gp0} \left[ \left( \frac{\alpha_{gp}}{L} \right) \frac{d\rho_{gp}}{dz} + \left( 1 + \alpha_{gp} \cdot \left( \frac{z}{L} \right) \right) \cdot \frac{d^2\rho_{gp}}{dz^2} \right] \quad (9)$$

Combining Equations 5 and 9 simplify

$$-E_{gp0} \left[ \left( \frac{\alpha_{gp}}{L} \right) \frac{d\rho_{gp}}{dz} + \left( 1 + \alpha_{gp} \cdot \left( \frac{z}{L} \right) \right) \cdot \frac{d^2\rho_{gp}}{dz^2} \right] + \frac{4}{d} \tau = 0 \quad (10)$$

Equation 10 is solved along with the boundary conditions: at  $z = 0$  (i.e. at the top of GPA)  $P = 0$  (Free boundary) and at  $z = L$  (tip of the GPA),  $P = P_0$  (the applied load). Equation 10 written in finite difference form reduces to

$$\left\{ \frac{\alpha_{gp}(\rho_{gp,i-1} - \rho_{gp,i+1})}{L} + (1 + \alpha_{gp} z'_i) \frac{(\rho_{gp,i-1} - 2\rho_{gp,i} + \rho_{gp,i+1})}{(\Delta z)^2} \right\} \frac{4}{E_{gpo} d} \tau_i = 0 \quad (11)$$

where  $\Delta z = (L/n)$  – length of differential element of GP. Rearranging the terms in Eq. 11

$$\frac{n^2}{L^2} \left\{ \frac{\alpha_{gp}}{2n} (\rho_{gp,i-1} - \rho_{gp,i+1}) + (1 + \alpha_{gp} z'_i) (\rho_{gp,i-1} - 2\rho_{gp,i} + \rho_{gp,i+1}) \right\} - \frac{4}{E_{gpo} d} \tau_i = 0 \quad (12)$$

Eq. 12 is written as

$$\left\{ a_i \cdot \rho_{gp,i-1} - 2b_i \cdot \rho_{gp,i} + c_i \cdot \rho_{gp,i+1} \right\} - \frac{4L^2}{n^2 \cdot E_{gpo} \cdot d} \tau_i = 0 \quad (13)$$

where  $a_i = \left( 1 + \alpha_{gp} z'_i - \frac{\alpha_{gp}}{2n} \right)$   $b_i = \left( 1 + \alpha_{gp} z'_i \right)$   $c_i = \left( 1 + \alpha_{gp} z'_i + \frac{\alpha_{gp}}{2n} \right)$

$a_i$ ,  $b_i$  and  $c_i$  are displacement influence coefficients.

$\rho_{gp,i}$  and  $\tau_i$  are respectively the displacement at the centre of node ‘i’ and the shear stress on the interface of element, ‘i’, of the GPA. Eq. 13 is written for nodes  $i = 2$  to  $(n-1)$ . Invoking the first boundary condition,  $P=0$  implies  $\sigma_z=0$  and hence strain,  $\epsilon_z=0$ , leads to i.e.,

$$\rho_{gp,1} = \rho_{gp,1'} \quad (14)$$

where  $\rho_{gp,1'}$ —displacement at the imaginary node 1’ above the GPA (Fig. 2a). Eqs. 13 and 14 are combined to arrive at the finite difference equation for node ‘1’, as

$$\left\{ a_1 \cdot \rho_{gp,1'} - 2b_1 \cdot \rho_{gp,1} + c_1 \cdot \rho_{gp,2} \right\} - \frac{4L^2}{n^2 \cdot E_{gpo} \cdot d} \tau_1 = 0 \quad (15)$$

Eq. 15 reduces to

$$\left\{ (a_1 - 2b_1) \rho_{gp,1} + c_1 \cdot \rho_{gp,2} \right\} - \frac{4L^2}{n^2 \cdot E_{gpo} \cdot d} \tau_1 = 0 \quad (16)$$

All the equations for nodes 1 to  $(n-1)$  are collated as

$$[L'_{gp}] \{ \rho_{gp} \} - \frac{4L^2}{E_{gp} \cdot n^2 \cdot d} \{ \tau \} = 0 \quad (17)$$

where  $[L'_{gp}]$  is the displacement coefficient matrix.

The pile displacements equations for nodes 1 to  $(n-1)$  are collated and summarized in Eq. 17. The pile displacement influence coefficients are

$$\begin{bmatrix} (a_1 - 2b_1) & c_1 & 0 & \dots & \dots & \dots & \dots & 0 \\ a_2 & -2b_2 & c_2 & 0 & \dots & \dots & \dots & 0 \\ 0 & a_3 & -2b_3 & c_3 & 0 & \dots & \dots & 0 \\ 0 & 0 & a_4 & -2b_4 & c_4 & 0 & \dots & 0 \\ \dots & \dots & \dots & \dots & \dots & \dots & \dots & \dots \\ \dots & \dots & \dots & \dots & \dots & \dots & \dots & \dots \\ \dots & \dots & \dots & \dots & \dots & \dots & \dots & \dots \\ \dots & \dots & \dots & \dots & \dots & a_{n-1} & -2b_{n-1} & c_{n-1} \end{bmatrix} \quad (18)$$

Considering the compatibility of displacements in soil and GPA

$$\{ \rho_s \} = \{ \rho_{gp} \} \quad (19)$$

Combining Eqs. 3 and 17 with Eq. 19

$$[L'_{gp}] \frac{d}{E_{so}} [L'_s] \{ \tau \} - \frac{4L^2}{E_{gpo} \cdot n^2 \cdot d} \{ 1 \} \{ \tau \} = 0 \quad (20)$$

where  $\{ 1 \}$  is the unit vector.

### 3 RESULTS AND DISCUSSION

Equation 20 is solved for the displacements in GPA. The displacements generated along the GPA length are extrapolated to obtain the top,  $\rho_0$ , and the tip,  $\rho_L$ , displacements considering the 1<sup>st</sup>, 2<sup>nd</sup> and 3<sup>rd</sup> elements for the top and  $n-2$ ,  $n-1$  and  $n^{\text{th}}$  elements for the tip displacements in the GPA, respectively. The results are presented for the following ranges of parameters.  $L/d$ : 5, 10, 25 and 50;  $K$ : 10 to 10,000; Poisson’s ratio,  $\nu_s$ : 0.5,  $\alpha_s = 0, 0.25, 0.5, 1$  and 2; and  $\alpha_{gp} = 0, 0.25, 0.5, 1$  and 2.

The influence of  $\alpha_s$  on the variation of the shear stresses with depth is presented in Figure 6 for  $L/d=10$ ,  $K=50$ ,  $\nu_s=0.5$  and  $\alpha_{gp}=0, 0.5$  and 1. The variations of the shear stresses with depth are magnified at top as shown in Figure 6(b). The variations of shear stresses with depth are very similar for both values of  $\alpha_s = 0$  and 0.5 and decrease with increasing values of  $\alpha_{gp}$ . The shear stresses at the tip decrease from 6.65 to 5.63 and from 5.25 to 4.39 for  $\alpha_s = 0$  & 0.5 with  $\alpha_{gp}$  increasing from 0 to 1 respectively. On the contrary, the shear stresses at the top increase from 0.35 to 0.41 and 0.77 to 0.86 for  $\alpha_s = 0$  & 0.5 with  $\alpha_{gp}$  increasing from 0 to 1 respectively.

The variations of shear stresses with depth as a function of  $\alpha_{gp}$  are presented in Figure 7 for  $L/d=10$ ,  $K=50$ ,  $\nu_s=0.5$  and for  $\alpha_s = 0, 0.5$  and 1.0. The plots are magnified for the stresses at the top in Figure 7(b). The variation of shear stresses with depth for  $\alpha_{gp} = 0$  & 0.5 are very similar for all  $\alpha_s$ .

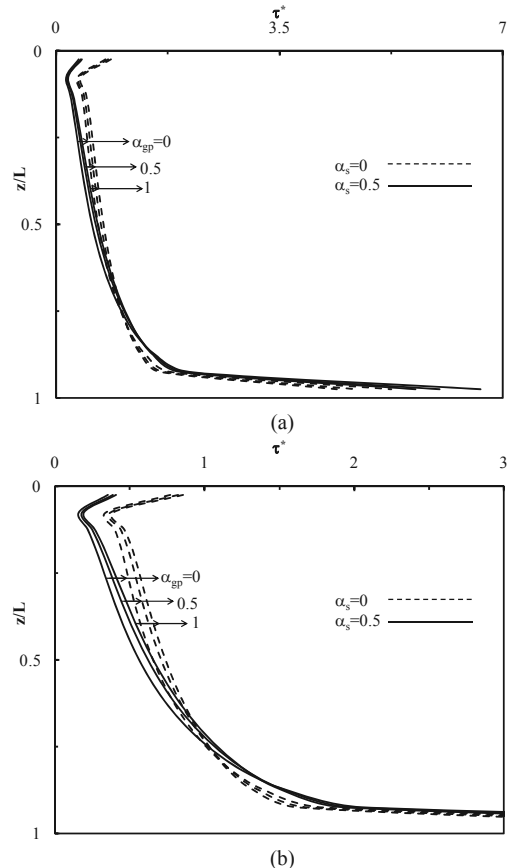


Fig. 6 Normalized shear stress,  $\tau^*$  vs. Depth,  $z/L$  for  $L/d = 10$ ,  $K=50$  &  $\nu_s=0.5$  – (a) Effect of  $\alpha_s$  &  $\alpha_{gp}$ . (b) Enlarged at top.

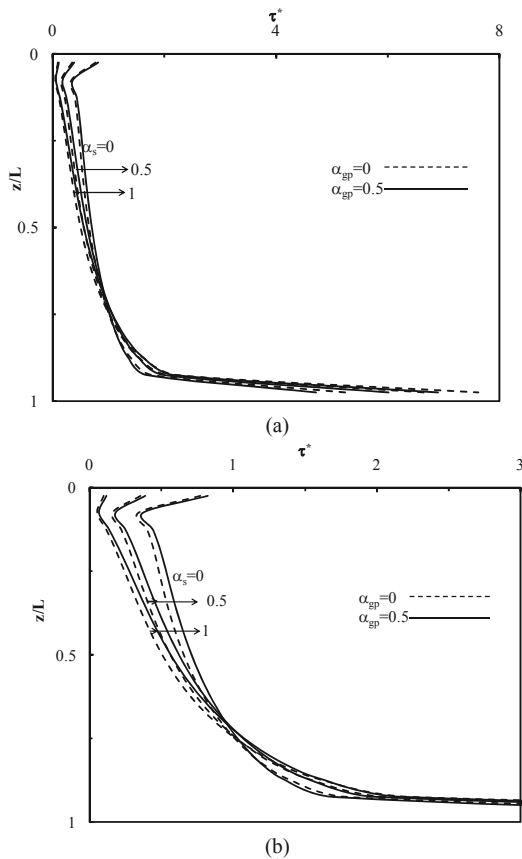


Fig. 7 Normalized shear stress,  $\tau^*$  vs. Depth,  $z/L$  for  $L/d = 10$ ,  $K=50$  &  $v_s=0.5$  – (a) Effect of  $\alpha_s$  &  $\alpha_{gp}$ . (b) Enlarged at top.

The variations of normalized tip displacements with depth for  $\alpha_s = 0$  ( $E_s$  constant with depth) and 0.5 are presented in Figure 8 for  $L/d=10$ ,  $K=50$ ,  $v_s=0.5$  and  $\alpha_{gp}=0, 0.5$  and 1. The displacement coefficients decrease with  $\alpha_{gp}$  at the tip, and increase at the top with  $\alpha_{gp}$  for  $\alpha_{gp}$  increasing from 0 to 1. The variation of  $I_U$  with depth is relatively large for smaller values of  $\alpha_{gp}$  compared to that for  $\alpha_{gp}=1$ . The displacement coefficient at the tip decreases from 1.91 to 1.47 for  $\alpha_s=0$  and from 1.732 to 1.34 for  $\alpha_s=0.5$ .  $I_U$  decreases by about 30% for  $\alpha_s=0.5$  in comparison to that for  $\alpha_s=0$  (homogenous soil).

The influence of  $\alpha_{gp}$ , the rate of increase of deformation modulus of granular material with depth on the variations of the displacement coefficients,  $I_U$  with depth for varying  $\alpha_s$  from 0 to 1,  $L/d=10$ ,  $K=50$  and  $v_s=0.5$  is presented in Figure 9. The displacement coefficient,  $I_U$ , for  $\alpha_s=0$ , at the tip decreases from 1.91 to 1.8 and increases from 1.12 to 1.17 for  $\alpha_{gp} = 0$  and 0.5 respectively. Similarly for  $\alpha_s=0.5$  and 1, the displacements at the tip decrease from 1.47 to 1.39 and 1.14 to 1.10 while at the top they increase from 0.87 to 0.90 and 0.71 to 0.74 for  $\alpha_{gp} = 0$  & 0.5 respectively.

#### 4 CONCLUSION

Analysis of the GPA under the influence of the non-homogeneities of the deformation moduli of the soil and granular material is presented in this paper. The shear stresses near the top of GPA are significantly less for  $\alpha_s$  increasing with depth. Displacements reduce for the deformation moduli parameters of soil and granular material increasing linearly with depth ( $\alpha_s=0.5$  &  $\alpha_{gp}=0.5$ ). The displacements reduce by 30% with depth for  $\alpha_s=0.5$  and 6% for  $\alpha_{gp}=0.5$  in comparison to those for  $\alpha_s=0$  and  $\alpha_{gp}=0$  respectively.

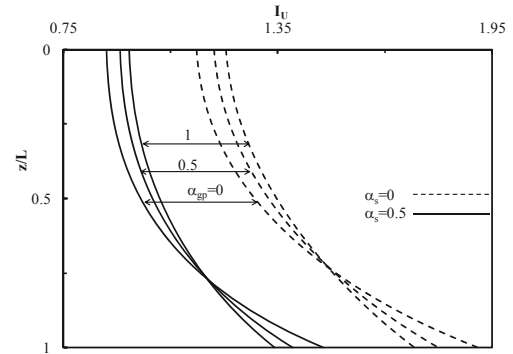


Fig. 8 Normalized displacement coefficient,  $I_U$  vs. Depth,  $z/L$  for  $L/d=10$ ,  $K=50$  &  $v_s=0.5$  – Effects of  $\alpha_s$  &  $\alpha_{gp}$ .

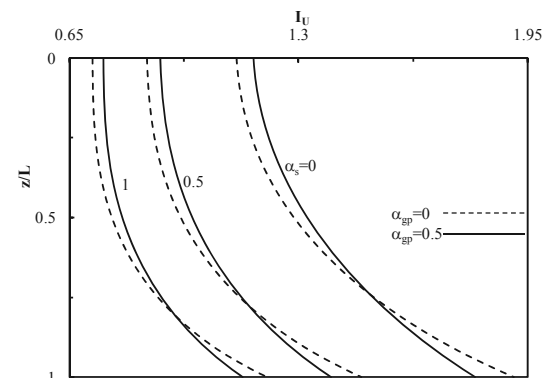


Fig. 9 Normalized displacement coefficient,  $I_U$  vs. Depth,  $z/L$  for  $L/d=10$ ,  $K=50$  &  $v_s=0.5$  – Effect of  $\alpha_{gp}$  &  $\alpha_s$ .

#### 5 REFERENCES

- Kumar P., Ranjan G. & Saran S. (2004). Granular Pile System for Strengthening of Weak Sub-Soils –A Field Study. International Conf. on Geosynthetics and Geov. Engg, Bombay, 217-222.
- Lillis, C., Lutenegeger, A.J & Adams, M. (2004). Compression and Uplift of Rammed Aggregate Piers in Clay. Geosupport: ASCE/GEO Geotechnical Special Publication no. 14, 497-507.
- Madhav, M.R., Vidyananya, B. & Sivakumar, V. (2008). Linear Analysis and Comparison of Displacements Granular Pile Anchors. J. Ground Improvement, Issue 161, 31- 41.
- Phanikumar, Sharma, R.S., Srirama Rao, A. & Madhav M.R. (2004). Granular Pile Anchor Foundation (GPAF) System for Improving the Engineering Behavior of Expansive Clay Beds. Geotechnical Testing J., ASTM, Vol.27(3), 1-9.
- Poulos, H.G. & Davis, E.H. (1980). Pile Foundation Analysis and Design. John Wiley and Sons, New York, 397.
- White, D., Wissmann, K., & Lawton, E. (2001). Geopier Reinforcement for Transportation Application. Geotechnical News : 63-68.